Modeling the Forces of Cutting with Scissors

Mohsen Mahvash, *Member, IEEE,* Liming Voo, Diana Kim, Kristin Jeung, Joshua Wainer, and Allison M. Okamura, *Associate Member, IEEE*

***Abstract*—Modeling forces applied to scissors during cutting of biological materials is useful for surgical simulation. Previous approaches to haptic display of scissor cutting are based on recording and replaying measured data. This paper presents an analytical model based on the concepts of contact mechanics and fracture mechanics to calculate forces applied to scissors during cutting of a slab of material. The model considers the process of cutting as a sequence of deformation and fracture phases. During deformation phases, forces applied to the scissors are calculated from a torque-angle response model synthesized from measurement data multiplied by a ratio that depends on the position of the cutting crack edge and the curve of the blades. Using the principle of conservation of energy, the forces of fracture are related to the fracture toughness of the material and the geometry of the blades of the scissors. The forces applied to scissors generally include high-frequency fluctuations. We show that the analytical model accurately predicts the average applied force. The cutting model is computationally efficient, so it can be used for real-time computations such as haptic rendering. Experimental results from cutting samples of paper, plastic, cloth, and chicken skin confirm the model, and the model is rendered in a haptic virtual environment.**

***Index Terms*—Haptic rendering, physics-based modeling, scissor cutting, biological tissues, robotics.**

I. Introduction

MODELING forces applied to surgical instruments is useful for surgical simulations and surgical planning [1]. Surgical simulators can provide a safe effective training environment, potentially reducing the use of human cadavers and animals [2]. Haptic technology is enabling the development of training simulators that allow users to feel tissue through virtual instruments. Realistic haptic feedback is expected to increase the training effectiveness of surgical simulators [3], [4]. To create realistic haptic surgical simulators, a high-fidelity approach is to calculate forces from physics-based models [5]. A physics-based model should relate the forces of simulation to either measured properties of a material or sampled force responses directly measured from mechanical interactions [6], [7].

Scissors are possibly the most effective and precise tools for cutting of thin tissues in open and laparoscopic surgery [8] and thin objects in daily tasks. To see this, compare cutting of a sheet of paper using a pair of scissors with that of using a sharp blade. When cutting with a blade, the paper should be firmly held, and it is difficult to make precise cuts. However, when cutting with a pair of scissors, the scissor blades themselves locally hold the paper, making it easy to have precise cuts.

An interaction between scissors and an object involves two main physical phenomena, local deformation and fracture. As soon as the scissors blades contact the object, the object is locally deformed. When the deformation reaches a certain level, fracture occurs and the object is separated. A physics-based model for scissor cutting should model forces of deformation and fracture.

It is generally impossible to directly calculate forces of local deformation of an object from its material properties and its constitutive equations in real time [9]. It takes a long time even for a very fast computer to calculate forces. However, since the forces of local deformations depend on only a few parameters, it is possible to calculate the forces from a few measured force responses using an analytical approach [9].

Fracture mechanics offers an energy-based approach to measure strength of an object against growth of cracks [10]. The basic idea is that the development of a crack inside an object requires a certain amount of energy that depends on the area of the crack and the fracture toughness of the object. Fracture toughness is a material property that defines the energy required to separate a unit of area of a material. Fracture toughness can also be interpreted as the resistance of a material against sharp cuts [10], [11].

In this paper, we use a fracture mechanics analytical approach to model forces applied to scissors during cutting of an object. The model calculates the forces from a measured torque-angle response, the fracture toughness of the object, the geometry of the scissors, and the position of the crack edge. Experimental results of cutting samples of paper, plastic, cloth, and chicken skin confirm the model, and a haptic virtual environment is used to demonstrate scissor cutting.

II. Related Work

Several approaches were used to model scissor cutting for haptic simulation. Greenish et al. used force data recording and replaying for haptic simulation of scissor cutting [12]. Only the information obtained during force recording could be replayed during simulation. Mahvash and Okamura introduced an analytical model to simulate cutting with scissors whose blades have a rectangular shape [13]. In this paper, we extend the analytical model to include scissors with arbitrary curves. We also perform experimental tests to verify the model.

Cutting of a deformable object is related to the fracture occurring inside the object [10], [11], [14], [15], [16], [17].

Manuscript received Nov 28, 2006. This work was supported in part by the National Science Foundation Grant No. EIA-0312551, National Institutes of Health Grant No. R01-EB002004, and the Johns Hopkins University.

M. Mahvash is with the Engineering Research Center for Computer Integrated Surgical Systems and Technology (ERC-CISST), the Johns Hopkins University, Baltimore, MD 21218 USA, (e-mail: mahvash@jhu.edu). A. M. Okamura is with the Department of Mechanical Engineering, the Johns Hopkins University, (e-mail: aokamura@jhu.edu). D. Kim, K. Jeung, and J. Wainer were with the Departments of Biomedical Engineering and Electrical and Computer Engineering, the Johns Hopkins University.

L. Voo is with The Johns Hopkins University Applied Physics Laboratory, Laurel, MD, 20723 USA, (e-mail: Liming.Voo@jhuapl.edu)

Darvell et al. introduced scissor cutting as an approach for measuring fracture toughness of thin deformable materials [15]. Pereira et al. used scissors to rank the fracture toughness of biological materials [16]. Ghatak and Mahadevan investigated the dynamics of a crack formed by a blunt cylindrical tool when it cuts a thin layer of a brittle material [18]. Mahvash and Hayward introduced a fracture mechanics approach for haptic rendering of cutting with a sharp tool [11]. The approach was applied to haptic rendering of cutting with a sharp blade. In [4], the fracture mechanics approach was extended to predict forces applied to a blunt laprascopic tool when it separated two deformable bodies. Heverly et al. investigated high-frequency force fluctuations caused during needle insertion [17]. Atkin et al. used an energy-based approach to explain why it is easier to cut with a sharp knife when pressing down and sliding (sawing) than pressing down alone [14].

Approaches that do not use fracture mechanics have been invoked to model cutting in surgical simulation and planning. For example, Chanthasopeephan et al. measured the force-displacement curve during cutting of a sample of liver with a sharp blade and used the finite-element method to model it. DiMaio and Salcudean developed a force model for needle insertion based on the finite-element method [19]. Okamura et al. developed a force model for needle insertion based on experimental data [20].

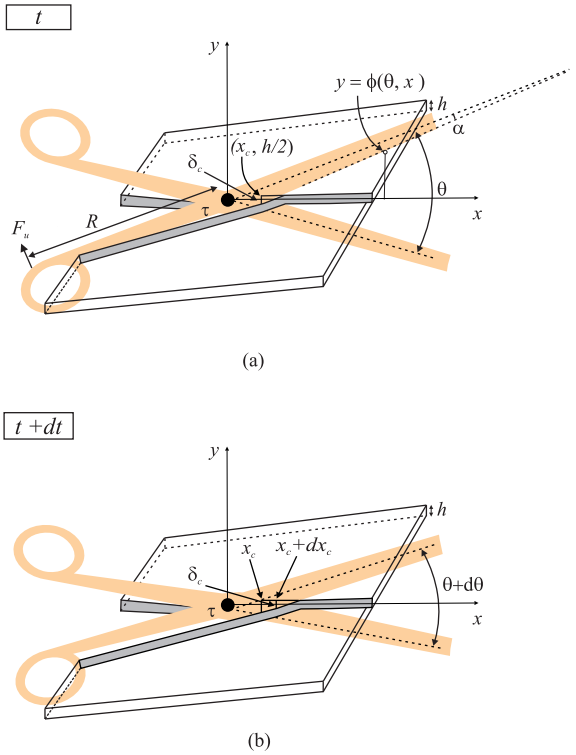

Fig. 1. The states of scissors and a plate at time t and $t + dt$ of a cutting process. At time t, the plate is locally deformed. During time period dt, a small area of the plate, $h\ dx_c$, is cut.

III. Scissor-Material Interaction Model

When you cut an object with a pair of scissors, the force that you feel between your fingers includes two main components: friction forces of the contact of the blades, and the forces of cutting of the object. In this section, we do not model the friction forces. However, we show in Section IV that friction forces can be measured by opening or closing empty scissors, and be summed into the model.

A. Contact Forces

Figure 1a shows the interaction between a pair of scissors and a thin plate with thickness h at the time t when the plate is locally deformed. A Cartesian frame is defined at the pivot of the scissors such that the x axis is along the symmetry line of the scissors. The plate is located along x and it does not move during cutting. We assume that the pivot of the scissors does not change orientation during cutting. For now, we also assume that the pivot of the scissors does not move. The opening angle of the scissors is defined by θ, and the position of the edge of the crack made by the scissors is defined by x_c.

The blades locally deform an area of the plate around the crack edge. The deformation can take various forms including bending, stretching, compression, or a combination thereof. During deformation, the upper edge of the crack tip is displaced from $(x_c, h/2)$ to $(x_c, h/2 - \delta)$, where δ is a displacement length (Figure 1). In response to deformation of the plate, the force f_n is applied to the upper blade along the normal to the blade's edge at point $(x_c, h/2 - \delta)$. f_n is calculated by

$$f_n = g(\delta), \tag{1}$$

where $g(\cdot)$ is a nonlinear function of the tip displacement, obtained by measurement or material properties.

The torque caused by f_n at the pivot is calculated by

$$\tau = x_c\ f_n \cos(\alpha), \tag{2}$$

where α is the angle between the blade's edge and the centerline of the blade. (α is not zero because scissors' blades are slightly tapered as shown in Figure 1.)

The force felt by the user at the handle is calculated by:

$$f_u = \frac{\tau}{R} = \frac{x_c}{R} f_n \cos(\alpha), \tag{3}$$

where R is the distance between the pivot and the handle.

B. Curve of the Blade Edge

The curve of the blade edge has a significant effect on the torque response of the scissors. Here, we define the curve of the edge of the upper blade in the Cartesian frame as

$$y = \phi(x, \theta), \tag{4}$$

where (x, y) is a point on the edge of the blade and $\phi(\cdot, \cdot)$ is a nonlinear function. We obtain ϕ by fitting an analytical curve to the edge of the upper blade as shown in Figure 2. We extract the blade edge from a real image of the blade.

Considering (4), the displacement length δ caused by a blade with curve ϕ is obtained by

$$\begin{aligned} h/2 - \delta &= \phi(x_c, \theta) \\ \delta &= h/2 - \phi(x_c, \theta). \end{aligned} \tag{5}$$

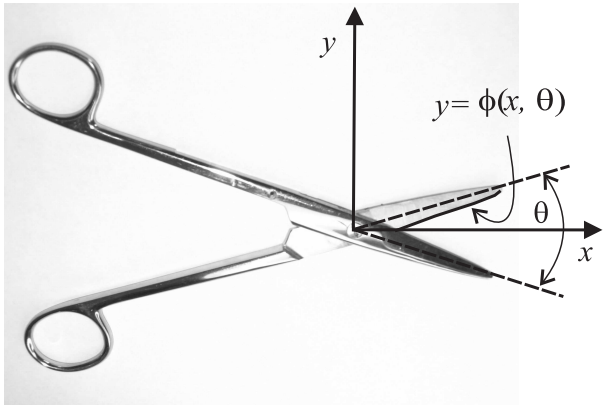

Fig. 2. Calculating blade curve ϕ for a pair of Metzenbaum scissors. An analytical curve is fit to the edge of the upper blade.

C. Sharp Cutting Forces

Figure 1 shows two sequential time steps: t, and $t + dt$, of a scissor cutting process. During dt, the opening angle of the scissors is changed from θ to $\theta + d\theta$, and the crack tip position is moved from x_c to $x_c + dx_c$. The area of crack extension is $dA = h\ dx_c$.

A fracture mechanics energy-based approach is used to estimate the torque and the crack tip position during cutting. Based on the principle of conservation of energy,

$$dW_e = dW_A + dU, \tag{6}$$

where dW_e is the external work applied by the scissors, dU is the change in elastic potential energy stored in the plate and dW_A is the irreversible work of fracture.

If we assume quasi-static operation and ignore inertia terms, the external work dW_e can be calculated by

$$dW_e = -\tau d\theta. \tag{7}$$

If the blade is very sharp such that it does not cause cutting burrs, the work of fracture for separating the area dA is calculated by [10]

$$dW_A = J_c\ dA = J_c\ h\ dx_c. \tag{8}$$

where J_c is the fracture toughness. Substituting (7) and (8) into (6) gives

$$-\tau d\theta = J_c h\ dx_c + dU, \tag{9}$$

and

$$\tau = -J_c h \frac{dx_c}{d\theta} - \frac{dU}{d\theta}. \tag{10}$$

If the deformation pattern around crack tip does not significantly change when the crack tip is displaced, we can ignore the change of the potential elastic energy stored in a plate during sharp cutting

$$\frac{dU}{d\theta} = 0. \tag{11}$$

This and (10) yield

$$\tau_c = -J_c\ h\ \frac{dx_c}{d\theta}. \tag{12}$$

where τ_c is the torque applied to the scissors during sharp cutting. $\frac{dx_c}{d\theta}$ is obtained by taking the derivative of (5) with respect to θ

$$\frac{d\delta}{d\theta} = \frac{1}{2}\frac{dh}{d\theta} - \frac{d\,\phi(x_c,\theta)}{d\theta} = 0 - \frac{\partial\phi}{\partial\theta} - \frac{\partial\phi}{\partial x_c}\frac{dx_c}{d\theta}. \tag{13}$$

If we ignore the change of displacement δ during cutting $\left(\frac{d\delta}{d\theta} = 0\right)$, we can conclude from (13)

$$\frac{dx_c}{d\theta} = -\frac{\partial\phi/\partial\theta}{\partial\phi/\partial x_c}. \tag{14}$$

Substituting (14) into (12) yields

$$\tau_c = J_c\ h\ \frac{\partial\phi/\partial\theta}{\partial\phi/\partial x_c}. \tag{15}$$

This shows that the torque during cutting depends on the toughness J_c, the thickness of the plate h, and the curve of the edges of the scissors $\phi(\cdot,\cdot)$, and it is independent of the stiffness of the plate represented by $g(\cdot)$.

D. High-Frequency Force Fluctuations During Cutting

High-frequency force/torque fluctuations are formed by a sequence of deformation and rupture phases caused inside the plate during cutting [11]. The torque increases during a deformation phase and overcomes the torque of sharp cutting. Then, the torque quickly drops when fracture occurs. The cutting model of this work does not predict the beginning of rupture phases and the amplitude of the force fluctuations. However, the model predicts the average torque during cutting where the torque fluctuates. Combining (10) and (12) yields

$$\tau = \tau_c - \frac{dU}{d\theta}. \tag{16}$$

An average torque is obtained by taking integrals from both sides of (10) during $[\theta\ \ \theta + \Delta\theta]$

$$\begin{aligned} \frac{\int_\theta^{\theta+\Delta\theta}\tau d\theta}{\Delta\theta} &= \frac{\int_\theta^{\theta+\Delta\theta}\tau_c d\theta}{\Delta\theta} - \frac{\int_\theta^{\theta+\Delta\theta} dU}{\Delta\theta}, \\ \tau_{\rm av} &\approx \tau_{\rm c} - 0 \end{aligned} \tag{17}$$

Thus the average torque is approximately equal to the torque of sharp cutting, and it is independent of deformation characteristics of the interaction.

E. Complete Scissor-Material Interaction Process

We summarize how the torque τ is calculated during a cutting process without force fluctuations. The following variables should be available to predict the whole scissor-material interaction: $g(\cdot)$, J_c, h, and $\phi(\cdot,\cdot)$. The interaction consists of different phases as marked in the torque-angle curve of Figure 3. From point 0 to point 1, the blades are not yet in contact with the plate so the torque is zero, $\tau = 0$. From 1 to 2, the blades deform a region around the crack tip x_c. The length of displacement at the crack tip, δ, is calculated by (5), and the torque τ is obtained by (2). When the level of τ reaches the sharp cutting torque τ_c, cutting starts, δ remains constant, and the crack tip x_c is updated by (5). At point 3, the scissors are opened, and the crack extension stops. From 3 to 4, the deformation at a new crack front relaxes, and

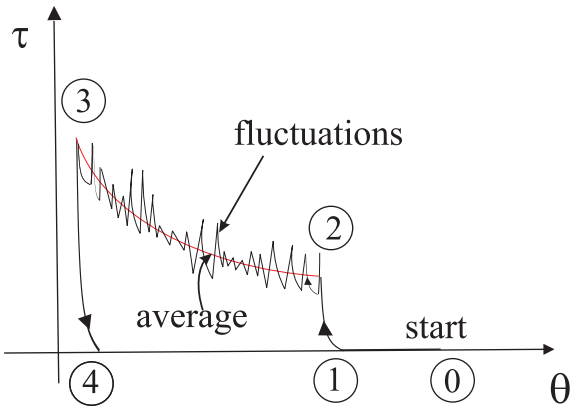

Fig. 3. Torque-angle responses of cutting processes with and without fluctuations. Each process consists of several phases: no contact, from 0 to 1, deformation, from 1 to 2, cutting, from 2 to 3, and deformation (relaxation), from 3 to 4 deformation. During the crack extension of cutting with fluctuations (from 2 to 3), the torque fluctuates around an average torque predicted by the cutting model.

the torque is calculated by (2). Figure 3 also shows another possible trajectory for scissor cutting. The torque trajectory includes high frequency fluctuations during fracture (from 2 to 3), which are not completely predictable. The high-frequency torque fluctuations are formed as a sequence of deformation and rupture phases. The average torque during 2 to 3 is predicted by (12).

F. Cutting by Slicing the Scissor Blades over the Plate

We now consider the case that the blades of the scissors slice through the plate to cut it. First, the scissor blades are closed and deform the plate. Then the pivot of the scissors are moved along x axis and cut the plate. The force caused by deformation force f_n (22) at the pivot along x is calculated by

$$f_x = -f_n \sin\left(\frac{\theta}{2} - \alpha\right) \tag{18}$$

where $\frac{\theta}{2} - \alpha$ is the angle between the upper blade edge and the x axis (Figure 1).

The torque applied to the upper blade is calculated by (2), considering x_c as the distance between the crack edge and the pivot. Sharp cutting starts when the torque reaches the sharp cutting torque level calculated by (15) and continues as long as the pivot moves toward the plate. The torque and force applied to the pivot remain constant during cutting if the opening angle of the scissors does not change.

IV. Experimental Validation of the Model

A series of cutting experiments were performed to validate the analytical model.

A. Methods and Materials

A two-degree-of-freedom robot holding a pair of scissors (Figure 4) was used to perform two sets of experiments, one set to obtain the parameters of the model and the other set to evaluate the model. The robot has a rotational arm and a translational arm that are able to close the scissors and move its pivot along a straight line. The pivot displacement and the opening angle were measured by encoders. An ATI Nano-17 force sensor attached to the rotational arm of the robot was used to measure the cutting forces. The force sensor was not connected to the upper blade, in order to prevent possible misalignments of the setup that would damage the force sensor.

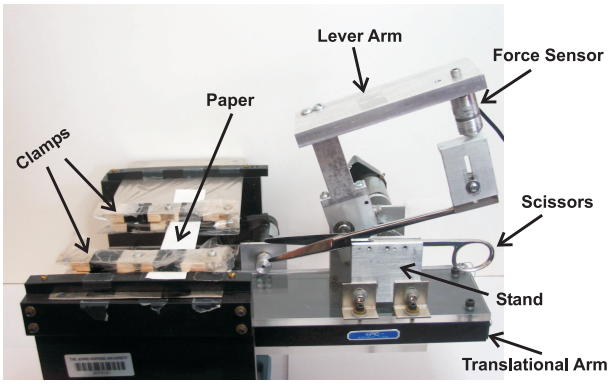

Fig. 4. A two-degree-of-freedom robot controls the motion of a pair of scissors to perform cutting. A force sensor measured forces applied to the handle.

Two pairs of Metzenbaum scissors with different blade sizes were used. The function that represents the edge curve of a pair of Metzenbaum was obtained by geometrical calculations (considering a blade has a tapered, rectangular shape, Figure 2):

$$\phi(x,\theta) = a + x\left(b + \frac{1}{2}\tan\left(\frac{\theta}{2}\right)\right), \tag{19}$$

where a and b were two constant coefficients. The coefficients for the small and large scissors were obtained based on measurements taken directly from the scissors. We took a picture of each pair of scissors and then set the coefficients fitting the curve $\phi(x,\theta)$ to the edge of the upper blade of the scissors in the image (Figure 2). The coefficients were:

$$\begin{aligned} &\text{Small scissors:} \quad a = -11,\ b = 0.14 \\ &\text{Large scissors:} \quad a = -11,\ b = 0.12 \end{aligned} \tag{20}$$

The distance of force sensor from the pivot of the scissors were

$$\begin{aligned} &\text{Small scissors:} \quad R = 9.8 \text{ cm} \\ &\text{Large scissors:} \quad R = 12 \text{ cm} \end{aligned}$$

These lengths were used to calculate torques applied to scissors from the forces measured by the force sensor.

We cut strips of four different materials: paper, plastic, cloth, and chicken skin. The width of all samples was approximately 2.3 cm. During each test, a sample was held along the straight edge of the upper blade of scissors by two clamps (Figure 4). The scissors were first opened by hand. Then a controller moved the pivot of the scissors to a certain distance from the edge of the sample, and closed the scissors at a rate of 3 degree/sec. The scissor pivot did not translate during cutting.

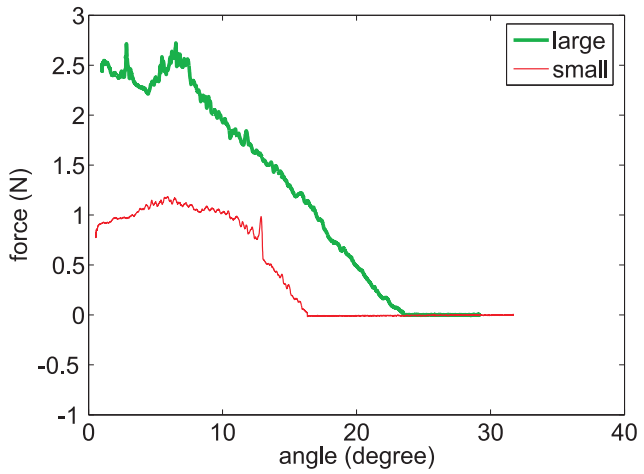

Fig. 5. The force-angle curves of empty cuts made by small and large scissors. The force curves show friction forces between the blades. The spike in force-angle response of the small scissors occurring around 12 degrees is due to a tiny nick on the surface of the upper blade of the scissors.

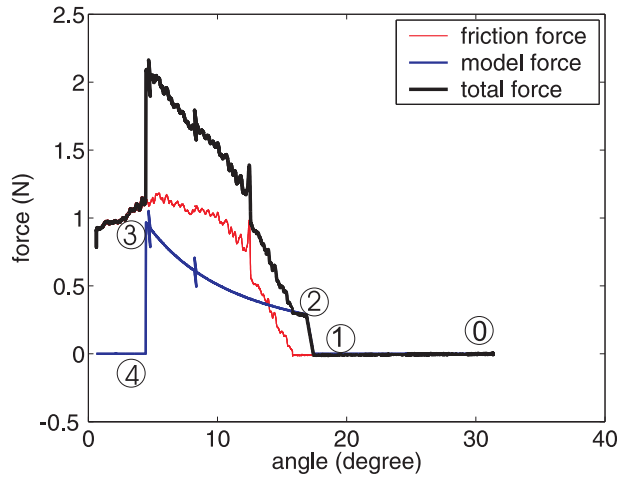

Fig. 6. The cutting model first calculates cutting forces during different phases, then the total forces are calculated by adding the cutting and friction forces. High-frequency force fluctuations in the total force curve are due to the force fluctuations of the empty cut curve (variation of friction forces). The plate ends at point 3 and therefore the force instantaneously declines and empty cut starts.

B. Model Parameters and Output

We obtained fracture toughness, J_c, and force-displacement curves of the plates, $g(\cdot)$, from a set of measurements obtained prior to evaluating the model. (Fracture toughness of materials can be alternatively found in material-property tables [14].) To obtain each parameter of the model, we performed five cutting tests on the same plate of material with the same scissors as described in the last section. We took the average of the five measurements to obtain the model parameters.

Friction between the blades of the pairs of scissors was measured by closing the blades over air (empty scissors), and was integrated into the model. Figure 5 shows the force-angle curves of empty cuts made by the small and large Metzenbaum scissors.

The fracture toughness of each plate for each test is obtained by

$$J_c = \frac{W_{\text{total}} - W_{\text{friction}}}{h l_c}, \tag{21}$$

where W_{total} is the external work applied to the scissors during cutting of the plate, W_{friction} is the external work applied to the scissors during the empty cut, and l_c is the length of cut.

W_{total} is calculated by the area under a measured force-angle curve multiplied by R, the distance between the force sensor and the scissors pivot. W_{friction} is calculated by the area under the force-angle curve of the empty scissors multiplied by R.

A linear function estimates $\mathrm{g}(\cdot)$, the force-deflection relationship during contact between a pair scissors and a plate.

$$\mathrm{g}(\delta) = k\ \delta, \tag{22}$$

where k is a constant factor. k depends on the elastic properties of the material (including Young's modulus and the shear modulus) and the sharpness of the scissors. We calculated k for each combination of material type and blade-cutting-edge sharpness from a force-deflection curve measured for an interaction between scissors of the same blade type and the plate of the same material during a deformation phase. Table I lists J_c of the four materials and k for deforming the four materials with the small scissors. We use the same k for the large scissors.

TABLE I
MODEL PROPERTIES OF THE FOUR DIFFERENT PLATES USED FOR SCISSOR CUTTING.

Material	J_c (KJ/m^2)	k (N/mm)	h (mm)
Paper	4.9	5	0.1
Plastic	3.17	20	0.1
Cloth	2.43	3	0.3
Chicken Skin	2.8	8	1.0

Figure 6 shows how the force-angle curve of cutting of a plate of paper is obtained using the analytical model. First, the cutting model calculates cutting forces during different phases of cutting based on the fracture toughness of the paper and k for the paper-small scissor combination. Then the total forces are calculated by adding the cutting forces and the measured friction forces.

C. Model Evaluation

We tested the following hypotheses about the analytical model through cutting the plates of the four materials:

- Force-angle curves of cutting of a slab of a material with a pair of scissors under the same model conditions are repeatable.
- The force-angle responses of cuts made with scissors match model predictions for various interaction situations.

Figures 7-10 each show three overlaid force-angle curves for cuts made by the small Metzenbaum scissors on plates of each of the four materials and the corresponding force-angle curve obtained by the analytical model. Figure 11 shows a force-angle curve of a cut made by the large Metzenbaum scissors

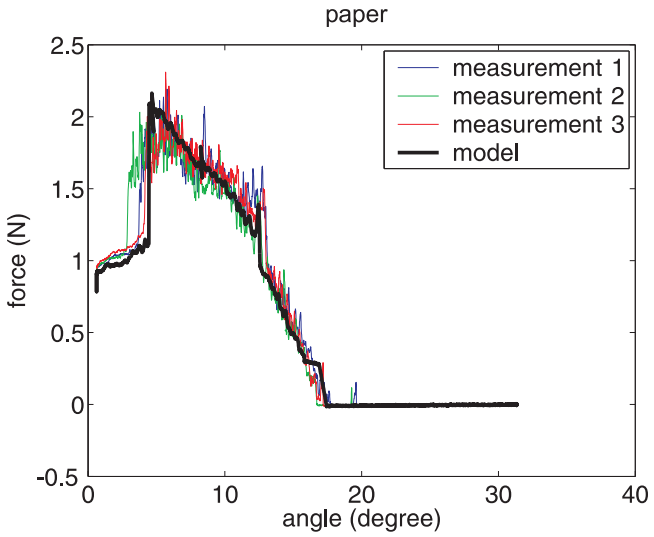

Fig. 7. Comparison of three force-angle curves made by the small scissors on *paper* samples and a force-angle curve obtained by the cutting model. Measured force-angle responses are similar. The model force response follows the average of the measured forces.

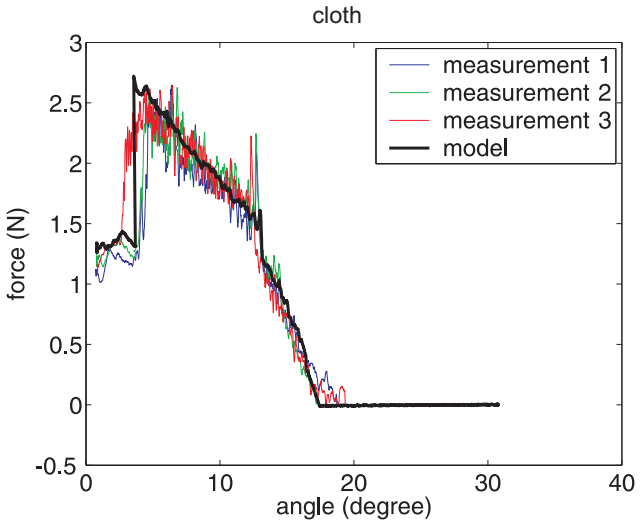

Fig. 9. Comparison of three force-angle curves made by the small scissors on *cloth* samples and a force-angle curve obtained by the cutting model. Measured force-angle responses are similar. The model force follows the average of the measured forces.

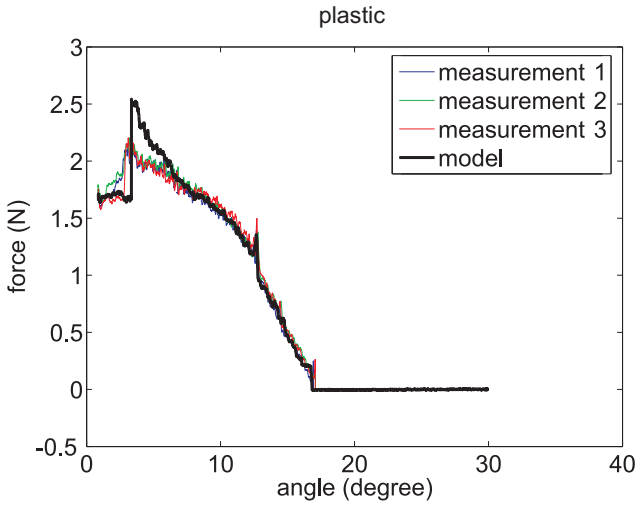

Fig. 8. Comparison of three force-angle curves made by the small scissors on *plastic* samples and a force-angle curve obtained by the cutting model. Measured force-angle responses are similar. The model force response follows the average of the measured forces.

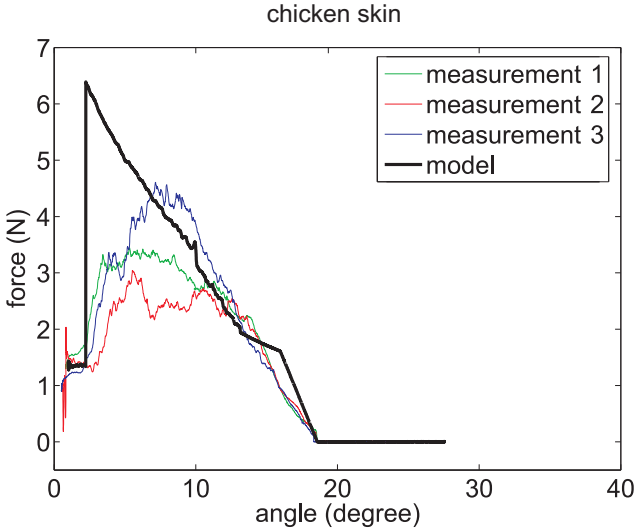

Fig. 10. Comparison of three force-angle curves made by the small scissors on *chicken skin* samples and a force-angle curve obtained by the cutting model. Measured force-angle responses are similar. The model force response follows the average of the measured forces during cutting for opening angles less than 7 degrees.

on a plate of paper and the corresponding force-angle curve obtained by the analytical model.

Referring to Figures 7-10, the measured force responses of each material are similar. They have the same phases (deformation and fracture) and the average force in each phase is almost equal to that predicted by the model. The force response of cutting chicken skin varied between samples more than the other materials. This is likely due to the thickness variation and inhomogeneity of chicken skin samples.

Figures 7-10 also show that the cutting model predicts cutting forces for various material toughness and contact stiffness. For most interactions shown in Figures 7-10, the cutting model forces are slightly larger than measured forces around the end of the cutting phase. The possible explanations for this are:

1) The edge curve of the blades near their ends or zero opening angle is not accurately estimated by the curve function ϕ.
2) The end of the plate was reached at the end of the cutting phase. At the end of the plate, the elastic energy stored in the plate no longer was fully shifted to a new crack edge. Instead, the elastic energy was gradually released in crack edge and this reduced the external energy and force required to make the cut.

It should be mentioned that the force responses of cutting chicken skin deviate significantly from the model toward the end of the cut. This is likely because all skin samples become thinner at the edges.

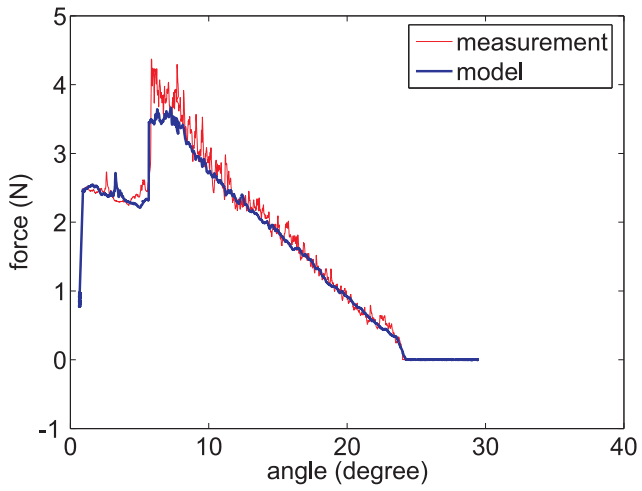

Fig. 11. Force-angle curves of cuts made by large scissors on paper. This confirms that the cutting model is valid for different scissors than the small scissors whose data are shown shown in Figures 7-10.

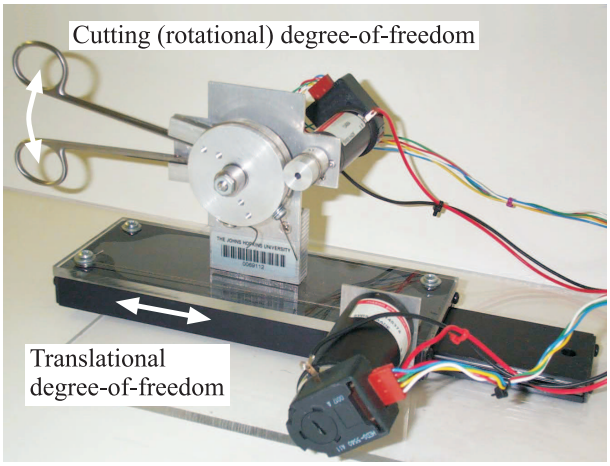

Fig. 12. Two-degree-of-freedom haptic scissors.

Figure 11 shows that the model accurately predicts the measured forces for the large scissors. This confirms that the cutting model is valid for different blade-edge curves, ϕ.

D. Evaluation of the Model for Haptic Rendering

The cutting model was used for haptic rendering of cutting with a pair of scissors in a virtual environment. The forces were rendered by the "haptic scissors", a haptic device developed in our laboratory (Figure 12) [21]. The haptic scissors can render forces in two degrees of freedom: translational and rotational. The cutting algorithm is updated at 1 kHz by a thread run under Windows 2000. The programmer can set the force-displacement curve of the contact, the toughness of the material, the thickness of the plate, and the curve of the blades.

The force returned by the haptic device consisted of two components which are computed separately and then added: the force representing sharp scissor cutting, and a friction force. The friction force due to contact of the scissor blades with each other is rendered using the stick-slide model of [22]. This model filters the measurement noise. The Coulomb friction level of the model (friction force during sliding phases of the model) is calculated by the empty-cut force-angle response of Figure 5.

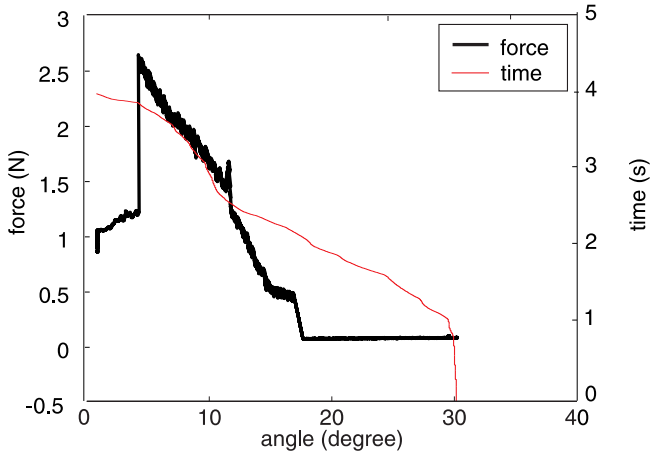

Fig. 13. During haptic simulation of scissor cutting of a layer of paper: force-angle and time-angle responses of the scissors. The model of Figure 7 was used to calculate forces.

Figure 13 shows the angle-time response and the force-angle output of the renderer when a layer of virtual paper was cut. In this example, the user only closed and opened the scissors, avoiding translation. The cutting model of Figure 7 was used to calculate forces.

We compare the force-angle curve of the simulation with the measured force-angle curves of cutting paper to evaluate the model for haptic rendering. The force-angle curve of simulation, Figure 13, has the same envelope as the predicted force-angle curve of Figure 7. Therefore, the envelope of the simulation force-angle curve is almost equal to the average of each experimental force-angle curve. This concludes that the frequency responses of the simulated force and each experimental force match at low frequencies.

Figure 13 shows force fluctuations with smaller amplitudes and lower frequency than the experimental data in Figure 7. Force fluctuations in Figure 13 are due to nonsmooth angular movement of the scissor blade, causing switching between deformation and fracture. Such nonsmooth motion will occur for any human user. Force fluctuations of Figure 7 might be due to nonhomogeneous material and rupture phases. Therefore, the frequency responses of the simulated force and experimental forces do not necessarily match at high frequencies.

A formal human subject test is beyond scope of this work, but users who tried the simulator expressed that the simulation realistically displayed the feeling of cutting homogeneous objects. This indicates that incorporating the force-fluctuations caused by rupture phases into the model may increase a user's ability to define the material type from simulation data.

V. Conclusions

We presented a computationally efficient analytical model to calculate the force-angle responses of cutting of a thin plate of a material with a pair of scissors. The model considered the process of scissor cutting as a time sequence of two different phases: deformation and sharp cutting. During

deformation phases, the force-angle responses were calculated by a measured force-angle curve multiplied by a ratio that depended on the location of the crack edge and the curve of the blades. A fracture mechanics approach based on the principle of conservation of energy calculated the forces during sharp cutting. The forces were obtained by the fracture toughness of the plate multiplied by a nonlinear function of the opening angle of the scissors and the position of the crack edge. The nonlinear function was obtained from the shape of the scissor blades. Experimental results from cuts on samples of four different materials confirmed the model. The model was rendered in a haptic virtual environment.

Future work will include precise modeling of force/torque fluctuations during cutting and investigating how they can be incorporated into haptic simulation.

REFERENCES

[1] H. Delingette, "Toward realistic soft-tissue modeling in medical simulation," *Proceedings of the IEEE*, vol. 86, no. 3, pp. 512–523, 1998.

[2] R. M. Satava, "Accomplishments and challenges of surgical simulation," *Journal of Surgical Endoscopy*, vol. 15, no. 3, pp. 232–341, 2001.

[3] C. R. Wagner, N. Stylopoulos, and R. D. Howe, "The role of force feedback in surgery: Analysis of blunt dissection," in *Proc. 10th Symp. on Haptic Interfaces for Virtual Environments and Teleoperator Systems*, 2002, pp. 68–78.

[4] M. Mahvash, "Novel approach for modeling separation forces between deformable bodies," *IEEE Transactions on Information Technology in Biomedicine*, vol. 10, no. 3, pp. 618–926, 2006.

[5] M. Mahvash and V. Hayward, "High fidelity haptic synthesis of contact with deformable bodies," *IEEE Computer Graphics and Applications*, vol. 24, no. 2, pp. 48–55, 2004.

[6] I. Browerand, J. Ustin, L. Bentley, A. Sherman, N. Dhruv, and F. Tendick, "Measuring in vivo animal soft tissue properties for haptic modeling in surgical simulation," *Studies in Health Technology and Informatics*, vol. 81, pp. 69–74, 2001.

[7] M. P. Ottensmeyer and J. K. Salisbury, "In vivo data acquisition instrument for solid organ mechanical property measurement," vol. 2208. Lecture Notes in Computer Science, Springer-Verlag, 2001, pp. 975–982.

[8] R. K. Mishra, "How do scissors work?" [Online]. Available: http://www.laparoscopyhospital.com/PR03.HTM.

[9] M. Mahvash, V. Hayward, and J. E. Lloyd, "Haptic rendering of tool contact," in *Proc. Eurohaptics*, 2002, pp. 110–115.

[10] A. G. Atkins and Y.-W. Mai, *Elastic and plastic fracture: metals, polymers, ceramics, composites, biological materials*, 1st ed. Chichester: Ellis Halsted Press, 1985.

[11] M. Mahvash and V. Hayward, "Haptic rendering of cutting, a fracture mechanics approach," *Haptics-e, the Electronic Journal of Haptics Research*, vol. 2, no. 3, November 2001.

[12] S. Greenish, V. Hayward, V. Chial, A. Okamura, and T. Steffen, "Measurement, analysis and display of haptic signals during surgical cutting," *Presence: Teleoperators and Virtual Environments*, vol. 6, no. 11, pp. 626–651, 2002.

[13] M. Mahvash and A. M. Okamura, "A fracture mechanics approach to haptic synthesis of tissue cutting with scissors," in *First Joint Eurohaptics Conference and Symposium on Haptic Interfaces for Virtual Environment and Teleoperator Systems (World Haptics)*, Pisa, Italy, March 2005, pp. 356–362.

[14] A. G. Atkins, X. Xu, and G. Jeronimidis, "Cutting, by pressing and slicing, of thin floppy slices of materials illustrated by experiments on cheddar cheese and salami," *Journal of Materials Science*, vol. 39, no. 8, pp. 2761–2766, 2004.

[15] B. W. Darvell, P. K. Lee, T. D. Yuen, and P. W. Lucas, "A portable fracture toughness tester for biological materials," *Measurement Science and Technology*, vol. 7, no. 6, pp. 954–962, 1996.

[16] B. P. Pereira, P. W. Lucas, and S.-H. T, "Ranking the fracture toughness of thin mammalian soft tissues using the scissors cutting test," *Journal of Biomechanics*, vol. 30, no. 1, pp. 91–94, 1997.

[17] M. Heverly, P. Dupont, and J. Triedman, "Trajectory optimization for dynamic needle insertion," in *Proceedings of the IEEE International Conference on Robotics*, Barcelona, Spain, 2005, pp. 1658–1663.

[18] A. Ghatak and L. Mahadevan, "Crack street: The cycloidal wake of a cylinder tearing through a thin sheet," *Physical Review Letters*, vol. 91, no. 21, p. 215507, 2003.

[19] S. P. DiMaio and S. E. Salcudean, "Needle insertion modeling and simulation," *IEEE Transactions on Robotics and Automation*, vol. 19, no. 5, pp. 864–875, 2003.

[20] A. M. Okamura, C. Simone, and M. D. O'Leary, "Force modeling for needle insertion into soft tissue," *IEEE Transactions on Biomedical Engineering*, vol. 51, no. 10, pp. 1707–1716, 2004.

[21] A. M. Okamura, R. J. Webster, J. T. Nolin, K. W. Johnson, and H. Jafry, "The haptic scissors: Cutting in virtual environments," in *IEEE International Conference on Robotics and Automation*, Taipei, Taiwan, September 2003, pp. 828–833.

[22] V. Hayward and B. Armstrong, "A new computational model of friction applied to haptic rendering," in *Experimental Robotics VI*, P. I. Corke and J. Trevelyan, Eds., vol. 250. Lecture Notes in Control and Information Sciences, Springer-Verlag, 2000, pp. 403–412.

Mohsen Mahvash received the Ph.D degree in electrical engineering from McGill University, Montreal, QC, Canada, in 2002. He was a postdoctoral fellow at The Johns Hopkins University, Baltimore, MD for two years. Mahvash is an assistant research professor at the Engineering Research Center for Computer Integrated Surgical Systems and Technology (ERC-CISST) at the Johns Hopkins University. His research interests include haptics, teleoperation, medical robotics, physics-based modeling, and control.

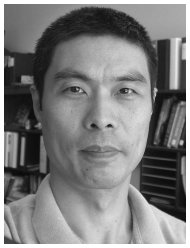

Liming M. Voo received his Ph.D. in Biomedical and Mechanical Engineering from the University of Iowa at Iowa City, Iowa in 1995. Dr. Voo has over 20 years of research experience in biomechanics related to injury, surgery, orthopedics, personal protection, and automotive safety. He is currently a Senior Research Scientist at the Johns Hopkins University Applied Physics Laboratory in Laurel, MD and an Associate Research Professor in the Department of Mechanical Engineering at the Johns Hopkins University, Baltimore, MD. Dr. Voo is a member of the American Society of Mechanical Engineers and an active member of its BioSolids committee.

Diana Kim received the B.S. degree in biomedical engineering from Johns Hopkins University, Baltimore, MD, in 2006.

Kristin Jeung received the B.S. degree in biomedical engineering from Johns Hopkins University, Baltimore, MD, in 2005.

Joshua Wainer received the B.S. degree in electrical and computer engineering from Johns Hopkins University, Baltimore, MD, in 2005

Allison M. Okamura (S'98 - A'00) received the B.S. degree from the University of California at Berkeley, and the M.S. and Ph.D. degrees from Stanford University, in 1994, 1996, and 2000, respectively, all in mechanical engineering. She is an Associate Professor of Mechanical Engineering at The Johns Hopkins University, Baltimore, MD. Her research interests include haptics, teleoperation, robot-assisted surgery, tissue modeling and simulation, rehabilitation robotics, and prosthetics. Dr. Okamura received a 2004 National Science Foundation CAREER Award, and the 2005 IEEE Robotics and Automation Society Early Academic Career Award.